Int. J. Electrochem. Sci., 11 **(2016)** 419 - 431

International Journal of
ELECTROCHEMICAL
SCIENCE
www.electrochemsci.org

Corrosion Resistance of Epoxy-Coated 3% Cr Steel in Saline Environment Measured Using EIS and SECM

K. Indira and T. Nishimura[*]

Materials Recycling Design group, Research Centre for Strategic Materials, National Institute for Materials Science (NIMS), Tsukuba, Ibaraki, Japan
[*]E-mail: NISHIMURA.Toshiyasu@nims.go.jp

Received: 6 October 2015 / *Accepted:* 6 November 2015 / *Published:* 1 December 2015

Electrochemical impedance spectroscopic (EIS) and scanning electrochemical microscopic (SECM) techniques are used primarily to evaluate the corrosion protection performance of epoxy-coated 3% Cr steel. Wet/dry cyclic corrosion tests (EIS) were performed on epoxy-coated carbon and 3% Cr steel samples in a 3 % NaCl solution. The EIS results showed that corrosion resistance of 3% Cr steel sample is greater than carbon steel sample. In order to determine the tip potentials for dissolution of Fe^{2+} and Cr^{2+}, cyclic voltammetry experiments were performed using the SECM tip at open circuit potential (OCP). The tip potential was set at -0.7, +0.04 and +0.60 V to determine the concentration of dissolved oxygen, and dissolution of Cr^{2+} and Fe^{2+} respectively. The dissolution of Fe^{2+} at the scratch defect was much lower in coated 3% Cr steel than in carbon steel. The consumption of oxygen was less for 3% Cr steel which is attributed to the fact that the dissolved oxygen reduction was decreased on the surface of 3% Cr steel compared to carbon steel. Thus, it was indicated that the weaker anodic and cathodic reactions were observed at the scratch of coated 3% Cr steel. In the case of dissolved oxygen, the tip current decreases for 3% Cr steel, which is ascribed to the reduction in the amount of dissolved oxygen over the sample surface. Corrosion resistance was much higher for the 3% Cr steel sample because the anodic and cathodic reactions at the scratch were weaker for coated 3% Cr steel than carbon steel.

Keywords: 3% Cr steel, epoxy coating, EIS, SECM, corrosion resistance

1. INTRODUCTION

Low alloy steels are the most economic, versatile and successful construction material used in steel structure. They have a long life; however, they will undergo corrosion eventually. Corrosion dramatically affects the performance of the structure, leading to heavy economic loss and safety problems.

Polymer coatings are used to protect the steels from corrosion by introducing a physical blockade between the steel surface and the corrosive environment [1, 2]. Corrosion occurs in the coated steel due to the formation of conductive pathways over the polymeric matrix where aggressive ions can diffuse from the electrolytic solution towards the unprotected surface area of the steel [3]. As the corrosion of coated carbon steel is very low, the potential use of low alloy steels, which have higher corrosion resistance, is attractive. However, there are few papers that investigate the corrosion of coated low alloy steels [4, 5]. Hence, it is necessary to apprehend the corrosion mechanism of coated low alloy steels.

In this context, electrochemical impedance spectroscopy (EIS) is a very powerful method for the detection of corrosion. However, conventional EIS is a macroscopic electrochemical technique that provides an averaged behavior of the entire surface [6]. Hence, the study of localized electrochemical reactions occurring in the metal surfaces is import to understand the corrosion process. In a coated steel surface, corrosion starts at defects in the coating. In these cases, a small active area has been formed within the cathodic region under the coating film by the local dissolution of metal [7]. Hence, it is necessary to determine the localized electrochemistry at the defect of the coating film.

Various techniques such as Scanning Vibrating Electrode Technique (SVET), Scanning Kelvin Probe (SKP), Scanning Electrochemical Microscopy (SECM), etc. are available to study the electrochemistry and corrosion process of the surface in the early stage at the microscopic level [8-10]. In the midst of these techniques, SECM is a very powerful method due to its high spatial resolution and electrochemical sensitivity to characterize the topography and redox activity of the metal/solution interface [11, 12]. In addition, its capability for *in-situ* measurement of the lateral distribution of the electroactive/chemical species (corrosion product) in the localized corrosion process with high lateral resolution would be highly advantageous [13, 14]. There are papers which already been reported the use of SECM in corrosion research for the detection of anodic and cathodic areas [9, 11], dissolution of metals [13], degradation of organic coatings [1-3], single pit generation [7], etc. [15].

Hence, in the present investigation, the EIS and SECM techniques are used primarily to evaluate the corrosion protection performance of low alloy steel samples with 3% Cr content used in concrete structures. The EIS and SECM experiments were performed on epoxy-coated carbon steel and 3 % Cr steel samples in a 3% NaCl solution.

2. EXPERIMENTAL PROCEDURE

2.1. Preparation of Steel Samples

The chemical composition of steel samples are given in Table 1. Three percent by mass Cr steel was mainly examined as a corrosion resistant steel; carbon steel was used for comparison. Silicon carbide papers of up to 1200 grit was used for polished the samples, then the sample surface was rinsed using distilled water and acetone and dried.

Table 1. Chemical composition of the samples

Sample	Elements (Mass %)									
	C	**Si**	**Mn**	**Cr**	**P**	**S**	**Al**	**N**	**O**	**Fe**
Carbon steel	0.1	0.2	1.0	-	0.01	0.003	0.01	0.001	0.002	bal
3% Cr steel	0.1	0.2	1.0	3	0.01	0.003	0.01	0.001	0.002	bal

2.2. Preparation of the Coating

The coating preparation was mentioned in an earlier report [8], the same procedure was followed in the present study. Fast-drying type epoxy resin was used in this present investigation. The liquid epoxy resin was a blend of multifunctional low molecular weight diluents and the diglycydal ether of bisphenol A, and the curing agent was based on aliphatic amines. The weight ratio of the epoxy resin to the curing agent was 2:1. The samples were coated with the help of a drawdown bar at constant speed; then kept at room temperature (25°C) for one week. This method led to the formation of 40 μm thick and uniform epoxy film coating on the steel surface. Artificial scratches (crosscut defects) were made in the coated samples.

2.3. EIS Measurements

A wet/dry cyclic corrosion test consisted of wetting the sample in a 3% NaCl solution for 12 h and drying the specimen at room temperature for 12 h. EIS measurements were done periodically in a 3% NaCl solution with three electrode system consisting of a scratched coated steel samples as the working and counter electrodes, and a saturated calomel electrode as the reference electrode. For the measurements with an amplitude of 10 mV over a frequency range of 40 kHz to 1 mHz, a frequency response analyzer was used. All the measurements were performed at open circuit potential (OCP) at room temperature. For analyzing the experimental data, curve fitting method was used.

2.4. CV Measurements

In order to fix the oxidation potential for Cr^{2+} and Fe^{2+} dissolution, the cyclic voltametric experiments were performed on SECM tip in a 3 % NaCl solution at a sweep rate of 0.01 V per seconds in OCP condition.

2.5. SECM Measurements

The SECM measurements were carried out over a large surface area i.e. 1000 μm^2 as a function of immersion time (0, 1, 3 and 7 h). SECM scan were acquired by rastering over the sample surface at steps of 50 μm in the Z-direction, 2500 μm in the Y-direction and 6000 μm in the X-direction. All the experiments were carried out at room temperature (25°C) in naturally aerated cell consisting of a 3% NaCl solution.

Fig. 1 shows the schematic representation of SECM instrument. This technique consists of an ultramicroelectrode (UME) tip that is placed inside an electrochemical cell and moves parallel to the sample surface to characterize the surface topography and redox activity of the solid/liquid interface [16]. In the present study, platinum microelectrode with diameter of µm was employed as the UME tip. The UME and the sample was biased independently as working electrodes with a bipotentiostat. A steady current (I) can be measured at the UME using the following equation (1) [9]:

$I = 4nFDC^*a \rightarrow (1)$

where, **a** denotes the radius of UME, **n** means the number of electrons participating in the redox reaction, **F** indicates the Faradaic constant, and **D** and **C** are diffusion coefficient and concentration of electroactive species in the bulk solution, respectively.

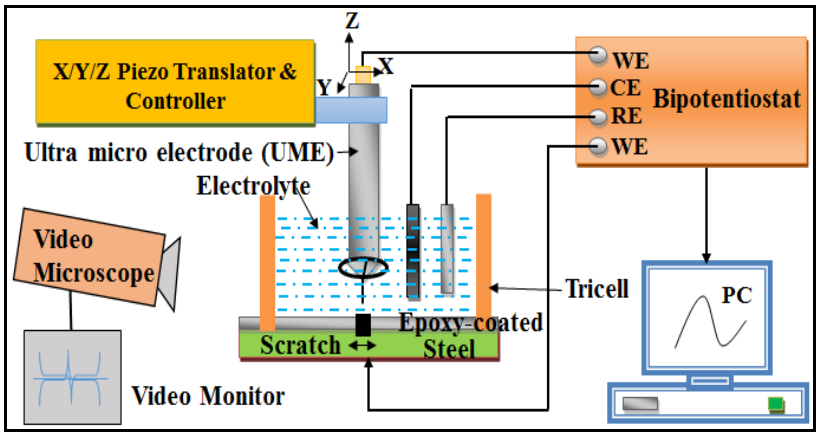

Figure 1. Schematic diagram of SECM

The tip movement was controlled in the X, Y and Z directions by means of an optically-encoded inchworm piezo meter. The Pt UME tip was scanned at a constant height directly above the sample surface when all experiments were executed. A video microscope was used for positioning the UME on the sample. All measurements were achieved using a Ag/AgCl reference electrode and Pt strip counter electrode. The testing was done during immersion in the electrolytic solution at the extemporaneously produced OCP of the sample. Coated sample was mounted horizontally at the bottommost of a micro flat cell thus baring the coated side upwards to test solution. A line scan was performed across the sample surface at a scan rate of 20 μms^{-1} in X-direction. Area scan (topographic mapping) was obtained in order to detect continuous changes in the corrosion at a constant height of 50 µm. All the 3 D maps shown were documented by fluctuating the UME tip from left to right.

3. RESULTS AND DISCUSSION

3.1. EIS Measurements

EIS measurements performed on scratched epoxy-coated carbon and 3% Cr steel samples after wet/dry cyclic corrosion test in a 3% NaCl solution for 15 days are shown in Fig. 2. In the Bode

diagram, there are 2 resistances and 1 capacitance in the spectrum. The EIS spectrum in high-frequency region is attributed to coating behavior, and the low-frequency region corresponds to corrosion reaction [17]. R_{sol} is constant at 0.02 – 0.05 kohmcm^2 in the 3% NaCl solution. Thus, the capacitance component is thought to be the double layer capacitance of the corrosion ($(C_{corr})^{\beta}$) at the steel surface. Two resistances in the spectrum are thought to be the coating resistance in the high-frequency region, and a charge transfer resistance (R_{corr}) in low-frequency region corresponds to corrosion reaction.

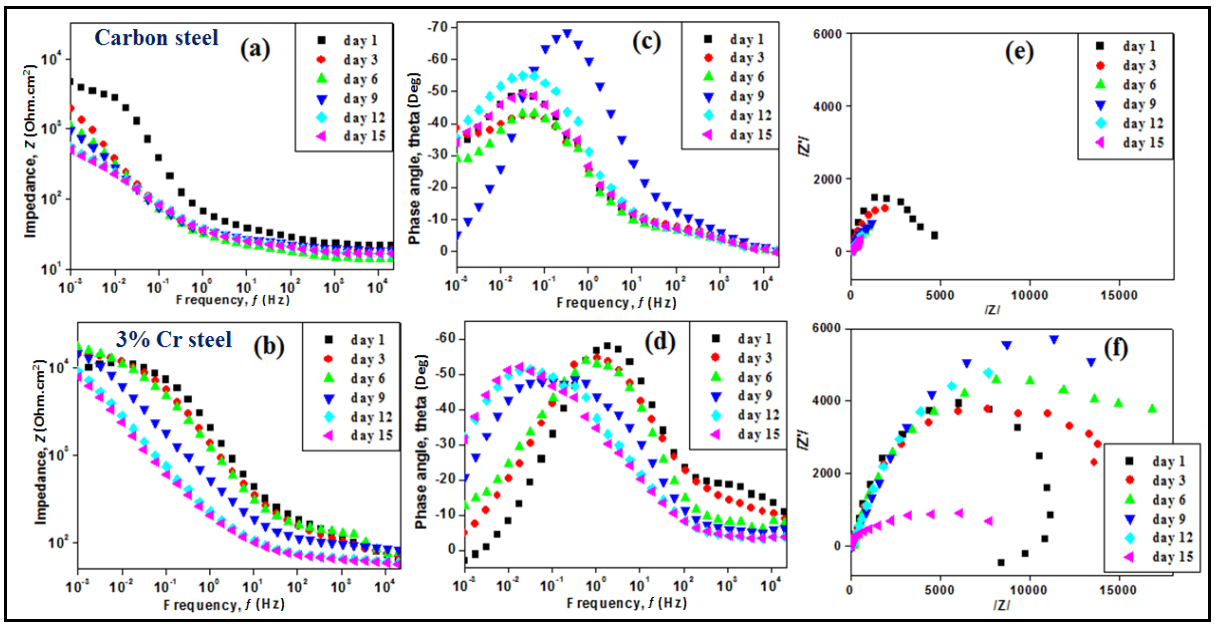

Figure 2. EIS plots of scratched epoxy-coated carbon and 3% Cr steel after wet/dry cyclic corrosion test in a 3% NaCl solution for various days: Bode Impedance plots (a-b), Bode phase angle plots (c-d) and Nyquest plots (e-f)

The shapes of the spectra are the same in the 3% Cr alloy steel and carbon steel (Fig. 2), and they are diminished with increasing test time, which indicates the progression of the corrosion of the coated steel. In more detail, the impedances (Z_{low}) in the low-frequency region are one order of magnitude higher for the 3% Cr alloy steel (Fig. 2b) than the carbon steel (Fig. 2a). Also, the Nyquest plots show that Z_{low} for carbon steel (Fig. 2e) is very much lower than the 3% Cr steel (Fig. 2f). These results show that 3% Cr steel can keep high corrosion resistance even though carbon steel has heavy corrosion during the test time.

All the EIS data in the present paper could be explained using the equivalent electrical circuit model displayed in Fig. 3 where R_{sol} denotes the solution resistance, R_{corr} indicates the charge transfer resistance corresponding to the corrosion reaction, C_f is the capacitance of the coating, and $(C_{corr})^{\beta}$ is the double layer capacitance of the corrosion reaction.

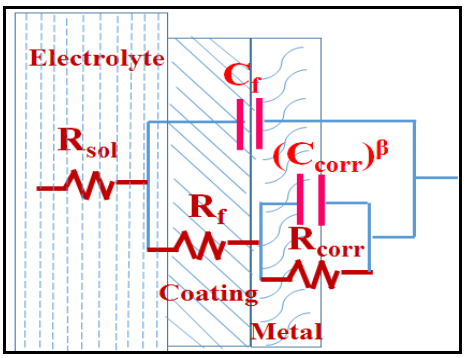

Figure 3. Equivalent circuit diagram for scratched epoxy-coated carbon and 3% Cr steel after wet/dry cyclic corrosion test in a 3% NaCl solution for various days

Fig. 4 displays the EIS parameters such as R_{corr}, R_f and $(C_{corr})^{\beta}$ obtained for the samples calculated from Fig. 2. For carbon steel, R_{corr} was 4.65 kohmcm^2 at 1 day, decreasing to 1.10 kohmcm^2 at 6 days, and further decreasing to 0.51 kohmcm^2 after 15 days whereas R_{corr} of 3% Cr steel was found to be 8.44 kohmcm^2 at 1 day, increasing to 17.30 kohmcm^2 at 6 days, and decreasing to 7.80 kohmcm^2 after 15 days.

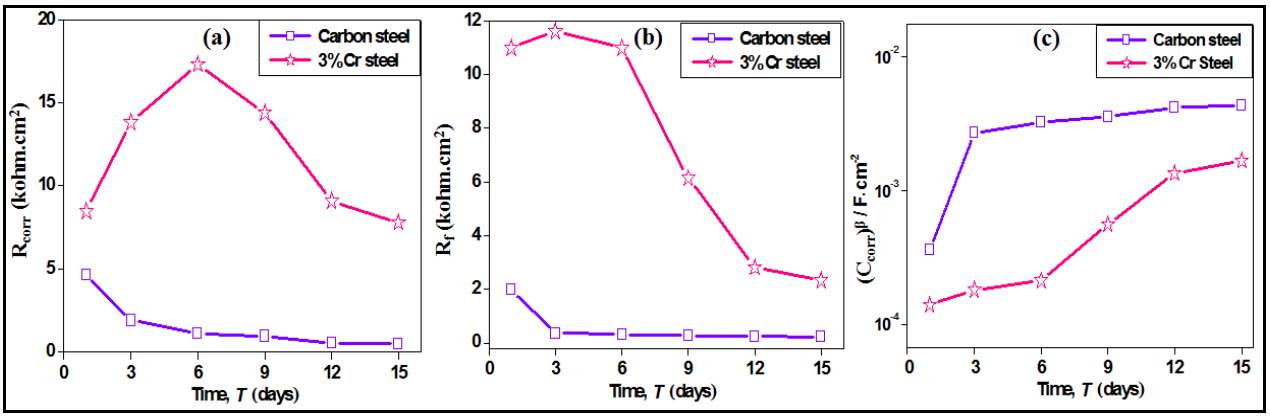

Figure 4. Impedance values of R_{corr} (a) , R_f (b), and $(C_{corr})^{\beta}$ (c) for scratched epoxy-coated carbon and 3% Cr steel after wet/dry corrosion test in 3% NaCl solution

Fig. 4b shows the change in R_f with time. The R_f values of carbon steel were 1.98 kohmcm^2 at 1 day, decreasing to 0.31 kohmcm^2 at 6 days, and further decreasing to 0.23 kohmcm^2 after 15 days whereas R_f of 3% Cr steel was 11.00 kohmcm^2 at 1 day, increasing to 11.00 kohmcm^2 at 6 days, and decreasing to 2.34 kohmcm^2 after 15 days. The higher R_f value of 3% Cr steel indicates the enhancement of barrier properties of the coating. The decrease in R_f values of carbon steel in the first few days was indicated the penetration of electrolyte through the coating [17]. It is vibrant from these resistance values that the 3% Cr steel is having higher corrosion resistance than carbon steel.

Fig. 4c shows the change in double layer capacitances, $(C_{corr})^{\beta}$ with time. The $(C_{corr})^{\beta}$ value of carbon steel was found to be low (on the order of 3.6 x 10^{-4} Fcm^{-2}) initially, then increased

progressively with immersion time attributable to the increase in corrosion area. After 15 days, the $(C_{corr})^{\beta}$ values for 3% Cr steel showed a lower value (0.001 x 10^{-4} Fcm^{-2}) compared to carbon steel (0.004 Fcm^{-2}). In carbon steel, the surface at the scratch is roofed with a less stable corrosion product (rust layer) through which Cl^- ions penetrated and touched the metal surface; hence, the corrosion begins at the scratch defect due to this process. However, at the scratch, the 3% Cr steel surface is roofed with a Cr rich corrosion product which suppresses of Cl^- ions penetration, thus, resulting in the reduction of $(C_{corr})^{\beta}$. On prolonged immersion, the carbon steel samples corrode more than the 3% Cr steel samples, and the EIS results are in accordance with the SECM results, given in the following sections.

3.2. SECM Measurements

The SECM analysis for the corrosion behaviors of epoxy-coated carbon and 3 % Cr steel samples was conducted to elucidate the corrosion processes in detail.

3.2.1 Cyclic Voltammetry analysis

Cyclic voltammetry is the ideal method for determining the electrochemical properties of any redox systems.

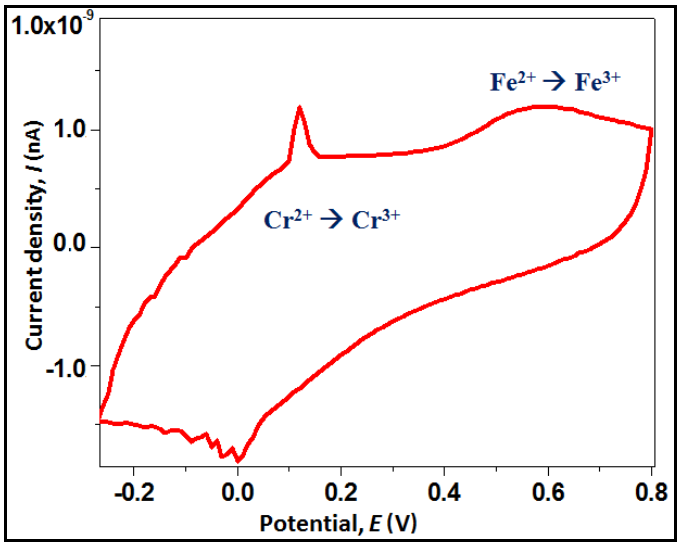

Figure 5. Cyclic voltagram for scratched epoxy-coated 3% Cr steel in 3% NaCl solution at OCP

Fig. 5 presents the cyclic voltagram of 3% Cr steel; the potential sweep was in the anodic path from –0.40 to +0.80 V, tailed by the cathodic sweep to -0.40 V at a sweep rate of 0.01 V per second. The initial current was found to be -1.95 nA at -0.40 V and it was increased to 1.00 nA at +0.80 V in the forward scan; the final current was -1.37 nA during the backward sweep. The forward sweep

(anodic direction) produces two limiting currents around at +0.01 - 0.04 V and 0.50 - 0.80 V, corresponding to the oxidation of dissolved Cr^{2+} to Cr^{3+} and Fe^{2+} to Fe^{3+} species, respectively. Kojijan et al. reported that at the potential anodic voltage of 0.00 V, Cr^{2+} would dissolve preferentially [18]. Based on the voltagram characterization, the probe potential was set at +0.04 V and +0.60 V vs. Ag/AgCl/KCl (3M) in order to monitor the dissolution of Cr^{2+} and Fe^{2+}, respectively, which are shown in the following sections as SECM topographic imaging and line scan analysis.

3.2.2. SECM topographic imaging

The variations in the chemical reactivity associated with the corrosion of epoxy-coated carbon and 3% Cr steel samples at their spontaneous OCP during immersion in a 3% NaCl solution were monitored using SECM. Fig. 6 shows the 3D maps of current distribution around the scratch (defect) obtained for Fe^{2+} dissolution set at 0.60 V in a 3 % NaCl electrolyte solution. An increase in the current is detected when the tip was skimmed over the metal surface (scratched area). This behavior is ascribed to the oxidation of Fe^{2+} to Fe^{3+} where the anodic dissolution of Fe^{2+} occurs at the steel [7]. In both samples, the current increases with increase in immersion time which indicates that the dissolution is greater with longer immersion times. Much less dissolution of Fe^{2+} is observed for 3% Cr steel than carbon steel which attributed to the higher resistance of the coated 3% Cr steel in the chloride environment.

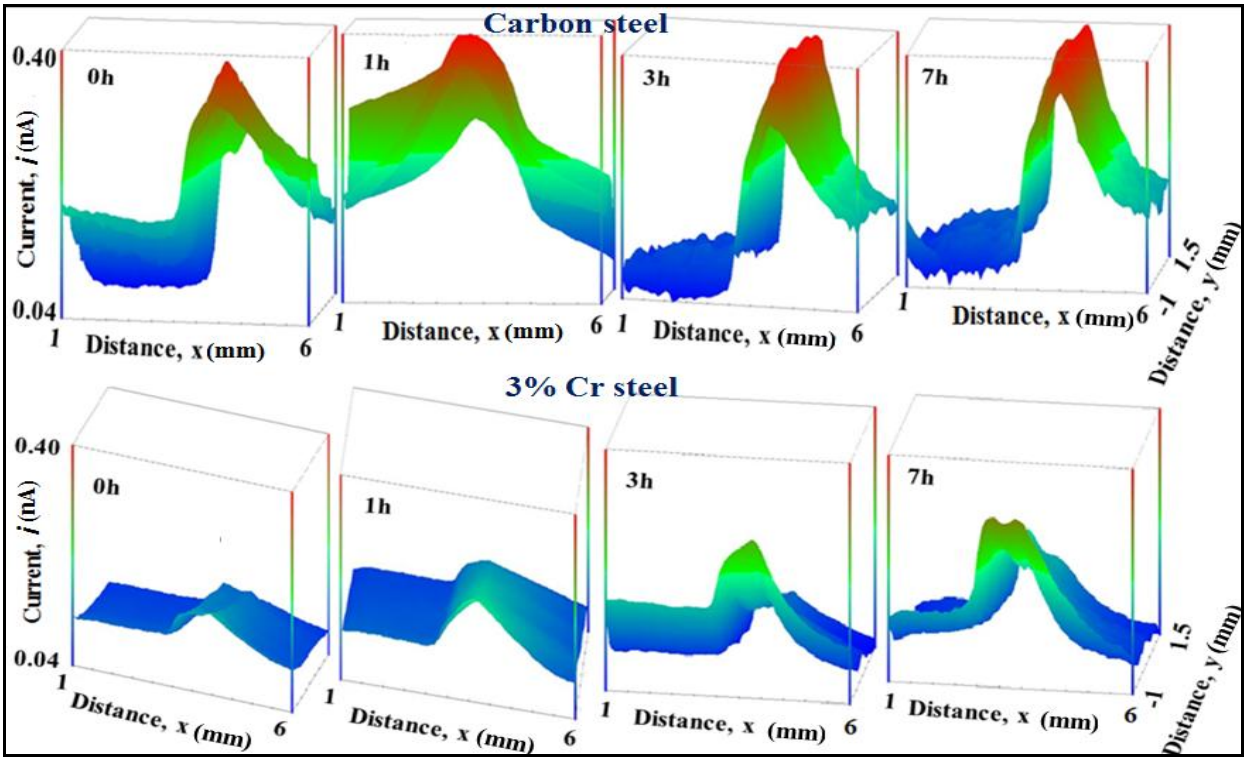

Figure 6. SECM 3D maps of surface topography obtained for scratched epoxy-coated carbon and 3% Cr steel in 3% NaCl solution at tip potential +0.60 V vs. Ag/AgCl/KCl reference electrode

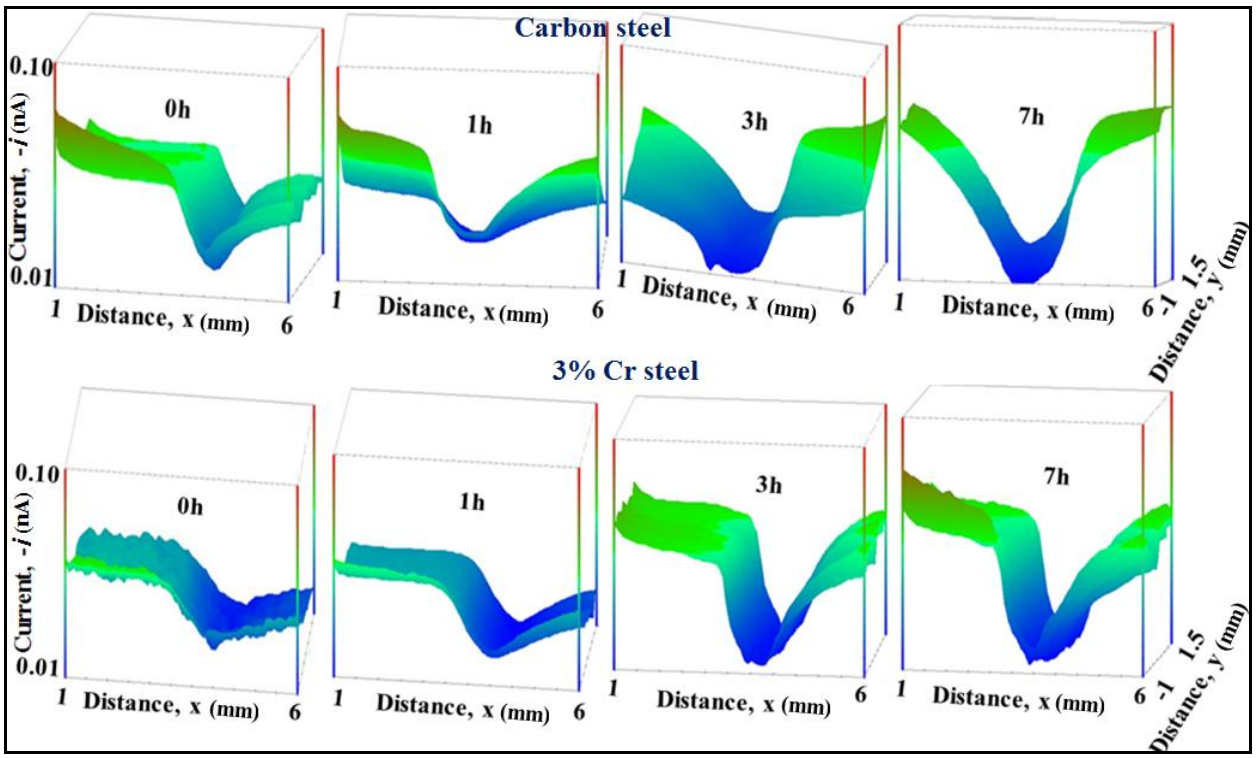

Figure 7. SECM 3D maps of surface topography obtained for scratched epoxy-coated carbon and 3% Cr steel in 3% NaCl solution at tip potential -0.70 V vs. Ag/AgCl/KCl reference electrode

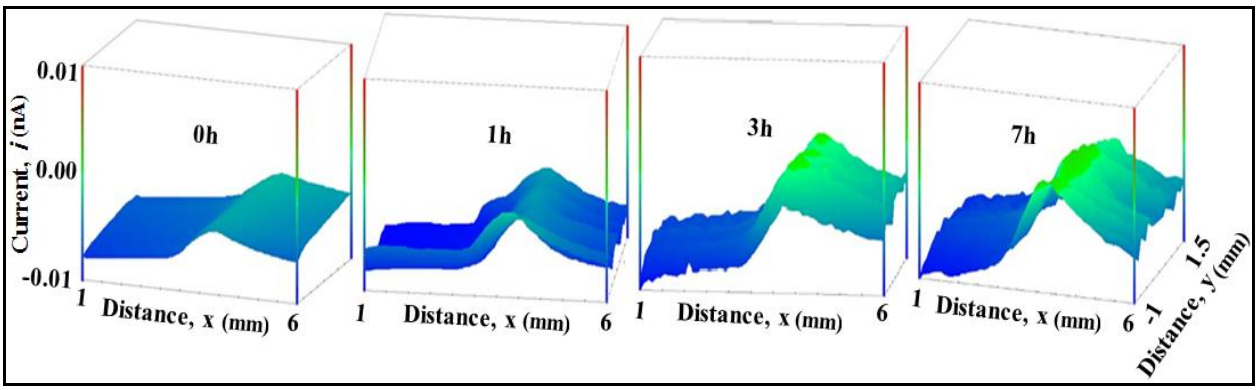

Figure 8. SECM 3D maps of surface topography obtained for scratched epoxy-coated 3% Cr steel in 3% NaCl solution at tip potential +0.04 V vs. Ag/AgCl/KCl reference electrode

The progress of the dissolved oxygen reduction can be followed by setting the tip potential at -0.70 V vs Ag/AgCl/KCl (3M). Fig. 7 shows the 3D maps of surface topography obtained for dissolved oxygen reduction in a 3 % NaCl solution. From the figure it is clear that the tip current is very high at the coated area and decreases near the scratched surface area. This behavior is thought to show that the consumption of oxygen occurs according to Fe^{2+}dissolution at the scratched surface area.

SECM measurements were done at the tip potential of 0.04 V vs. Ag/AgCl/KCl (3M) in a 3 % NaCl electrolyte solution to monitor the Cr^{2+} dissolution. Fig. 8 shows the 3D maps of surface topography obtained for Cr^{2+} dissolution. Higher current is observed at the scratched area than at the intact coated surface. The current increases with immersion time which indicates higher dissolution of

Cr^{2+} with extended immersion time. Although the Cr^{2+} dissolution is low as compared to Fe^{2+} (Fig. 6), the dissolution of Cr^{2+} also increases with time.

3.2.3. SECM line scan analysis

Fig. 9 shows the line scan images obtained for Fe^{2+} dissolution and reduction of dissolved oxygen in 3 % NaCl electrolyte solution. For 3% Cr steel, Fe^{2+} dissolution took place gradually with increasing immersion times as shown in Fig. 9b, whereas in carbon steel, the Fe^{2+} dissolution is drastic with increasing immersion times (Fig. 9a). Thus, higher current is observed for carbon steel than for 3% Cr when the line scan was achieved at the tip potential of +0.60 V that indicates higher Fe^{2+} dissolution occurs in carbon steel than in 3% Cr steel. Similarly, the reduction of dissolved oxygen is drastic with immersion time in carbon steel (Fig. 9c) and gradual in the 3% Cr steel (Fig. 9d). Greater current decreases are observed for carbon steel (Fig. 9c) than for 3% Cr steel (Fig. 9d) when the line scan was performed at the tip potential of -0.70 V which indicates higher oxygen consumption due to anodic dissolution of Fe^{2+} in the carbon steel.

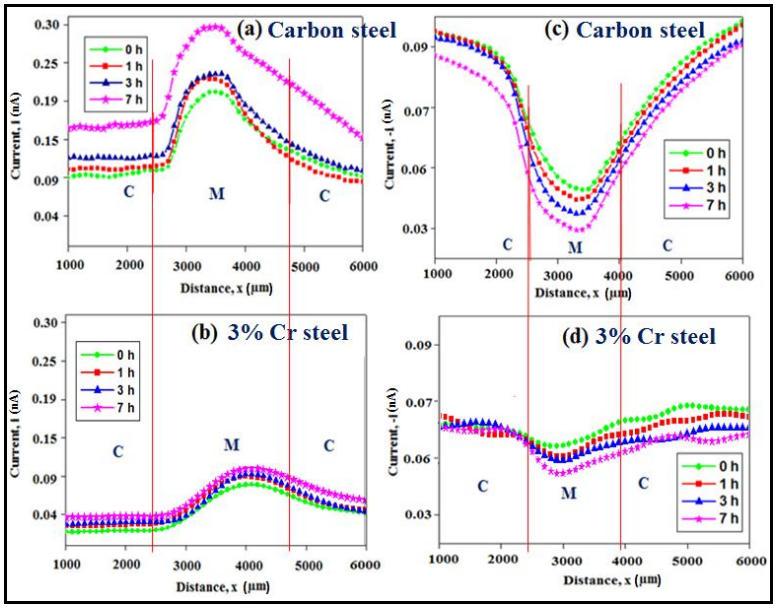

Figure 9. SECM line scan images of scratched epoxy-coated carbon and 3% Cr steel in 3% NaCl solution at tip potential: +0.60 V (a-b) and -0.70 V (c-d) vs. Ag/AgCl/KCl reference electrode

Maximum current is calculated from Figs. 9a and 9b which is illustrated in Fig. 10a. A gradual increase in i_{max} from 0.086 to 0.090 nA for 0 to 7 h is observed for 3% Cr steel, whereas, in the carbon steel, a drastic increase in the current from 0.211 to 0.295 nA is observed with increasing immersion times. This behavior shows Fe^{2+} dissolution is more rapid in carbon steel than in 3% Cr steel.

Minimum current is calculated from Figs. 9c and 9d shown in Fig. 10b. At the initial time (0h), i_{min} is smaller for carbon steel (-0.039 nA) than for 3% Cr steel (-0.058 nA). In both carbon and 3% Cr

steel samples, i_{min} increases from -0.053 to -0.039 nA and -0.065 to -0.058 nA, respectively with increase in immersion time.

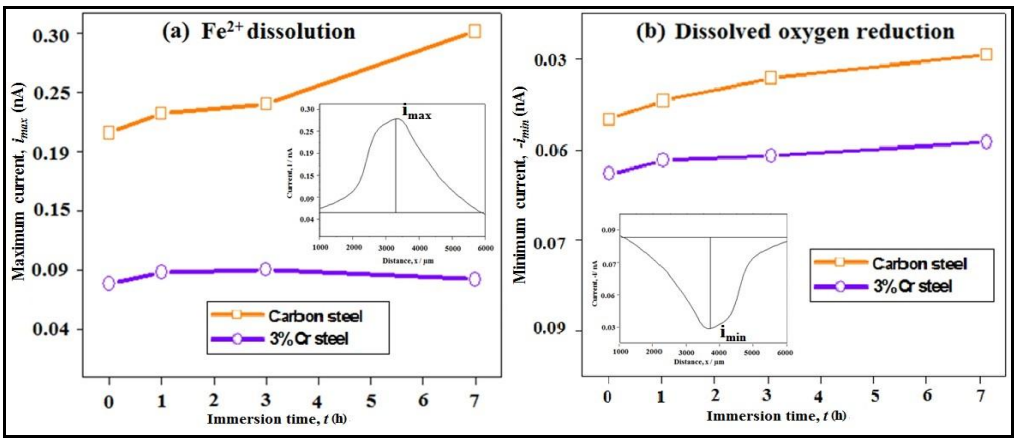

Figure 10. (a) Maximum current at tip potential +0.60 V vs. Ag/AgCl/KCl reference electrode and (b) minimum current at tip potential -0.70 V vs. Ag/AgCl/KCl reference electrode

Fig. 11a shows the line scan images obtained for Cr dissolution in a 3 % NaCl electrolyte solution. As seen in the earlier cases, the current at the scratched area is higher than at the unscratched coated area.

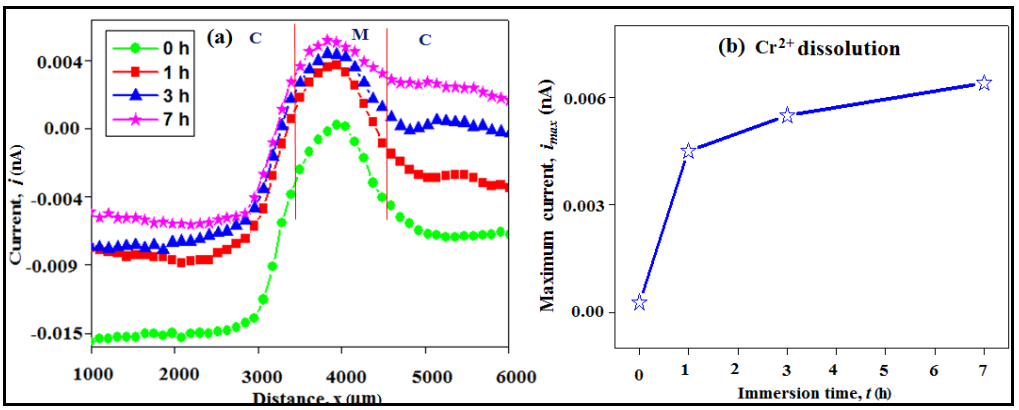

Figure 11. (a) SECM line scan images of scratched epoxy-coated 3% Cr steel in 3% NaCl solution at tip potential 0.04 V and (b) maximum current at tip potential +0.04 V vs. Ag/AgCl/KCl reference electrode

Maximum current calculated from Fig. 11a is shown in Fig. 11b. An increasing current trend from 0.0002 to 0.0063 nA is observed with increase in immersion time. The current is for the Cr^{2+} dissolution is much lower than for Fe^{2+} dissolution which means the iron dissolves more than chromium in oxide electrolyte interface. This is because the content of chromium in the steel is much lower than iron content.

3.2.4. Corrosion mechanism of coated 3 % Cr steel

A corrosion protection mechanism at the scratched area of epoxy-coated 3 % Cr steel may be proposed based on above results, and contains two parts as follows:

The first part of the mechanism is concerning the SECM measurement in this study.

The dissolution of Fe^{2+} at the scratch was much less in coated 3% Cr steel than in carbon steel. The consumption of oxygen was less for 3% Cr steel which is attributed to the fact that the dissolved oxygen reduction was less at the surface of 3% Cr steel than at carbon steel. Thus, it was indicated from SECM that weaker anodic and cathodic reactions were observed at the scratch of coated 3% Cr steel.

The dissolved oxygen depletion in the electrolyte solution as a significance of the cathodic process occurring on the steel surface can be measured using SECM [19]. The main cathodic reaction taking place during corrosion process is the dissolved oxygen reduction as given in the reaction:

$O_2 + 2H_2O + 4e^- \rightarrow 4\ OH^- \rightarrow$ (1)

The oxygen reduction reaction plays a vital role in the passivation process of the metal by producing the local current that polarizes the metal into the passive region [20].

If the steel sample contains chromium, then $Cr(OH)_3$ can precipitate over the sample surface that reduces the electrical conductivity and increases the cation selectivity of the corrosion products. This kind of hydroxide, like passive film, can block penetration of anions like Cl^- and decrease the anionic concentration at the interface. Specially, as the $[OH^-]$ increases by the oxygen reduction reaction at the scratch, the formation of $Cr(OH)_3$ is promoted. Thus, in SECM measurement, the anodic reaction can be repressed which resulting in decrease of corrosion process [21].

The second part of the mechanism is concerning the EIS measurement in this study.

The metal surface is progressively blocked by the precipitation of chromium- and iron-containing corrosion products thus resulting in enhanced resistance of the surface. It is reported elsewhere [22] that the enrichment of Cr^{2+} and depletion of Fe^{2+} could be observed at the metal-oxide interface. In other words, the chromium level decreases and the iron level increases near the oxide-electrolyte interface. The enrichment of chromium in the rust layer acts as a barrier to the corrosion process. Furthermore, the atomic diameter of chromium is similar to iron, and both atoms have same valence electron number, thus, the chromium can partly substitute for iron and forms a new $Cr_xFe_{1-x}OOH$. Such a rust layer is equipped with cation selective ability with the result of suppressing the passage of Cl^- ions [23].

Thus, the reason for the superior corrosion resistance of 3% Cr alloy steel is the formation of stable and/or insoluble Cr containing oxide (spinel $FeCr_2O_4$), which forms an uninterrupted network of Cr-O-Cr-O thus preventing Fe^{2+} dissolution [18]. From the above two parts of the mechanism, it is clear that the epoxy coated 3% Cr steel has greater corrosion resistance in a chloride containing environment and can potentially be used as construction material in concrete structures.

4. CONCLUSIONS

The corrosion protection behavior of epoxy-coated carbon and 3% Cr steel was assessed primarily using EIS and SECM techniques. EIS results revealed that the epoxy-coated 3% Cr steel

exhibited higher corrosion resistance than carbon steel. The SECM tip potential was set at -0.7, +0.04 and +0.60 V determining out the concentration of dissolved oxygen and dissolution of Cr^{2+} and Fe^{2+}, respectively. SECM results indicated that less Fe^{2+} dissolution and less oxygen reduction were observed at the scratch of coated 3% Cr steel than at the carbon steel. From the above results, it is clear that the coated 3% Cr steel sample exhibited superior corrosion resistance in the wet/dry cyclic corrosion test in a chloride-containing solution than carbon steel. This behavior is attributed to the fact that the anodic and cathodic reactions at the scratch were much less active for coated 3% Cr steel than for carbon steel.

References

1. R.M. Souto, Y.G. Garcia and S. Gonzalez, *Corros. Sci*., 47 (2005) 3312.
2. R.M. Souto, Y.G. Garcia, S. Gonzalez and G.T. Burstein, *Electroanalysis*, 21 (2009) 2569.
3. R.M. Souto, Y.G. Garcia, J. Izquierdo and S. Gonzalez, *Corros. Sci*., 52 (2010) 748.
4. S.A. Park, S.H. Lee and J.G. Kim, *Met. Mater. Int.*, 18 (2012) 957.
5. S.A. Park, W.S. Ji and J.G. Kim, *Int. J. Electrochem. Sci.*, 8 (2013) 7498.
6. B.B. Katemann, A. Schulte, E.J. Calvo, M.K. Hep and W. Schuhmann, *Electrochem. Commun*., 4 (2002) 134.
7. C. Gabrielli, S. Joiret, M. Keddam, N. Portail, P. Rousseau and V. Vivier, *Electrochim. Acta*, 53 (2008) 7539.
8. X. Joseph Raj and T. Nishimura, *ISIJ International*, 54 (2014) 693.
9. A.M. Simoes, A.C. Bastos, M.G. Ferreira, Y.G. Garcia, S. Gonzalez and R.M. Souto, *Corros. Sci*., 49 (2007) 726.
10. A. Madhankumar, N. Rajendran and T. Nishimura, *J. Coat. Technol. Res*., 9 (2012) 609.
11. A.C. Bastos, A.M. Simoes, S. Gonzalez, Y.G. Garcia and R.M. Souto, *Electrochem. Commun.*, 6 (2004) 1212.
12. S. Gao, Dong, H. Luo, K. Xiao, X. Pan and X. Li, *Electrochim. Acta*, 114 (2013) 233.
13. K. Fushimi and M. Seo, *Electrochim. Acta*, 47 (2001) 121.
14. J. Izquierdo, L.M. Ruiz, B.M.F. Perez, L.F. Merida, J.J. Santana and R.M. Souto, *Electrochim. Acta*, 134 (2014) 167.
15. J. Izquierdo, J.J. Santana, S. Gonzalez and R.M. Souto, *Electrochim. Acta*, 55 (2010) 8791.
16. J.J. Santana, J.G. Guzman, L.F. Merida, S. Gonzalez and R.M. Souto, *Electrochim. Acta*, 55 (2010) 4488.
17. A. Madhankumar, S. Nagarajan, N. Rajendran and T. Nishimura, *J. Solid State. Electrochem*, Doi 10.1007/s10008-011-1623-1, 2011.
18. A. Kojijan, C. Donik and M. Jenko, *Mater. Technol*., 43 (2009) 195.
19. Y.G. Garcia, S.J. Garcia, A.E. Hughes and J.M.C. Mol, *Electrochem. Commun.*, 13 (2011) 1094.
20. R.L. Garcia, R. Akid, D. Greenfield, J. Gittens, M.J.M. Portero and J.G. Anton, *Electrochim. Acta*, 70 (2012) 105.
21. Q. Wu, Z. Zhang, X. Dong and J. Yang, *Corros. Sci*., 75 (2013) 400.
22. N. Ramasubramanian, N. Procanin and R.D. Davidson, *J. Electrochem. Soc*., 132 (1985) 793.
23. Q. Zhang, J. Wu, W. Zheng, J. Wang, J. Chen, X. Yang and A. Li, *J. Mat. Sci. Technol*., 8 (2002) 455.